Synthesis and Proton Transfer-linked Redox Tuning of Ruthenium(II) Complexes with Tridentate 2,6-Bis(benzimidazol-2-yl)pyridine Ligands

Xiao Xiaoming,[a] Masa-aki Haga,*[,b] Takeko Matsumura-Inoue,[a] Yu Ru,[c] Anthony W. Addison*[,c] and Kenji Kano[d]

[a] *Nara University of Education, Takabatake-cho, Nara, Japan*
[b] *Department of Chemistry, Faculty of Education, Mie University, 1515 Kamihama, Tsu, Mie 514, Japan*
[c] *Chemistry Department, Drexel University, Philadelphia, PA 19104, USA*
[d] *Gifu Pharmaceutical University, 6-1 Mitahora-higashi 5, Gifu 502, Japan*

New ruthenium complexes of two tridentate ligands 2,6-bis(benzimidazol-2-yl)pyridine (L^7) and 2,6-bis(1-methylbenzimidazol-2-yl)pyridine (L^8) have been synthesised. Proton and ^{13}C NMR spectroscopy served well for their characterization, and the observed change. Proton chemical shift yields information about the electron distribution accompanying deprotonation of the ligands. The $[RuL^7_2]^{n+}$ chelate acts as a tetrabasic acid, with pK_a ranging from 2.5 to 10.7, depending on the ruthenium oxidation state. The absorption spectra and oxidation potentials are consequently sensitive to solution pH and to solvent. The proton-coupled oxidative electron-transfer reactions of the complexes afford stable higher oxidation states such as Ru^{IV}. The properties of the complexes are discussed in comparison to those of previously reported bis(tridentate ligand)ruthenium compounds.

The modification or fine tuning of the electronic and redox properties of ruthenium(II) complexes is required for the design of supramolecular systems intended for photochemical molecular devices for energy conversion and photoinduced electron transfer.[1] However, most studies have been limited to complexes involving bidentate ligands such as 2,2'-bipyridine (bipy). Over the past decade quite a large amount of data has been accumulated on the changes in the electrochemical and chemical properties of complexes effected by substitution in the bipy rings or replacement of one or both of the pyridine rings by other nitrogen-containing heterocycles.[1,2] On the other hand, there are relatively fewer ruthenium complexes with tridentate ligands.[3] Few ligands other than 2,2':6',2''-terpyridine (L^1, terpy) have been used in this regard until quite recently, because the synthesis of substituted terpyridines is quite difficult. Recently, several new tridentate ligands, L^2–L^6, have been used in order to modify the properties of the resulting complexes and to elucidate the directed electron-transfer reaction within a conformationally rigid system.[4] 2,6-Bis(pyrazol-1-yl)-pyridine (L^3) has been synthesised to modify the properties and reactivity of ruthenium complexes.[5] It has been reported to be both a weaker π acceptor and a weaker σ donor than L^1. In addition, tridentate ligands, which provide ligand environments different in composition and symmetry from those of bidentate ligands, may prove to be advantageous for application in asymmetric catalysis[6] or reactive oxidant generation.[7]

In the present study we report the use of the tridentate ligands 2,6-bis(benzimidazol-2-yl)pyridine (L^7) and 2,6-bis(1-methylbenzimidazol-2-yl)pyridine (L^8) to synthesise a new series of ruthenium(II) complexes. The benzimidazolyl group is a strong σ donor compared to 2-pyridyl or pyrazolyl. Furthermore, coordination can be expected to increase the ease of dissociation of the benzimidazole NH imino protons [equation (1)], so that the physical and chemical properties of the ruthenium complexes with L^7 may consequently be regulated by proton-transfer equilibria. The oxidation states Ru^{III} and Ru^{IV} are easily accessible through the proton-transfer linked redox chemistry of $[RuL^7_2]^{2+}$.

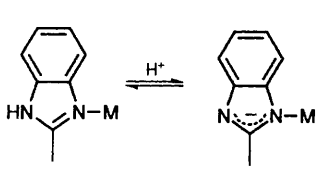

(1)

Experimental

Materials.—Reagents were used as received from Aldrich, Eastman-Kodak, Fisher and Wako, and used without further purification unless otherwise stated. Tetra-*n*-butylammonium

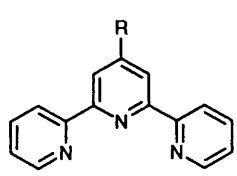

L^1 R = H
L^2 R = C_6H_4Me-*p*

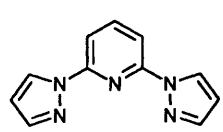

L^3

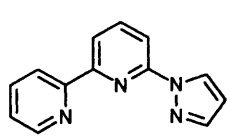

L^4

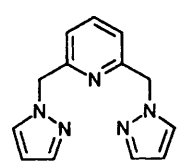

L^5

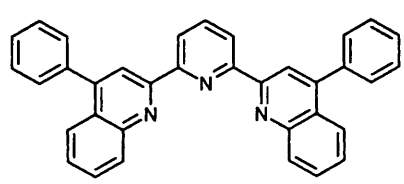

L^6

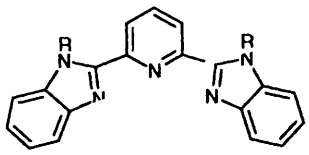

L^7 R = H
L^8 R = Me

hexafluorophosphate was prepared by the metathesis of KPF_6 with NBu_4Br in water, purified by recrystallization from ethyl acetate–pentane, and dried over P_4O_{10} *in vacuo*. Tetraethylammonium perchlorate from G. F. Smith Chemical Co. was recrystallized from water and dried similarly. Acetonitrile was dried over P_4O_{10}, and then CaH_2, and distilled from one of these reagents under N_2 (boil-off from MG Industrial Gases liquid N_2). Dimethylformamide (dmf) was vacuum-distilled from CaH_2. Water used in spectrophotometric and electrochemical measurements was deionized and then distilled using an all-glass apparatus. The buffer systems and pH ranges employed were as follows: $HClO_4$–$NaClO_4$, pH 0–2; Britton-Robinson buffer (H_3PO_4–H_3BO_3–$MeCO_2H$–NaOH), pH 2–11.

Preparations.—The ligands L^7 and L^8 were prepared according to the literature procedures.[8]

$[RuL^7_2][PF_6]_2$. Ruthenium(III) chloride trihydrate (0.22 g, 1 mmol) and L^7 (0.62 g, 2 mmol) were refluxed in 95% ethanol for 2 d. After cooling, the solution was filtered and KPF_6 (1 g, 5.4 mmol) was added. The olive precipitate was collected, washed with EtOH, and dried *in vacuo* at 155 °C (60% yield) (Found: C, 44.3; H, 2.75; N, 13.5. Calc. for $C_{38}H_{26}F_{12}N_{10}P_2Ru$: C, 44.2; H, 2.70; N, 13.6%).

$[RuL^7_2][ClO_4]_2$. **CAUTION:** Perchlorate salts are potentially explosive. Although no explosions were experienced while working with this system, a tiny quantity on a microspatula in a flame showed its explosive tendency so the handling of only small quantities is recommended. Ruthenium(III) chloride trihydrate (1.25 g, 5.5 mmol) was heated in glycerol (50 cm^3) under nitrogen for 1 h at 150 °C until the solution became green. To the resulting solution was added solid L^7 (3.12 g, 10 mmol) and the mixture was heated for 5 h at 200 °C. After dilution of the resulting solution with water (100 cm^3), $NaClO_4$ (0.91 g, 5.6 mmol) was added to give an olive-brown precipitate, which was collected and recrystallized from methanol (50% yield) (Found: C, 47.3; H, 3.05; N, 13.3. Calc. for $C_{38}H_{26}Cl_2N_{10}O_8Ru{\cdot}2H_2O$: C, 47.6; H, 3.15; N, 14.6%).

$[RuL^8_2][PF_6]_2$. Ruthenium(III) trichloride trihydrate (0.22 g, 1 mmol) and L^8 (0.73 g, 2.14 mmol) were refluxed in 95% ethanol for 2 d and allowed to cool. A saturated aqueous solution of KPF_6 (4 cm^3) was added and ethanol was removed *in vacuo* to induce precipitation. The residue was dissolved in toluene–acetonitrile (1:1) and chromatographed on silica gel using the same solvent as eluent. The yellow first band was discarded. Concentration of the second band yielded a solid, which was redissolved in acetonitrile (3 cm^3). Reprecipitation was induced by adding diethyl ether (200 cm^3), and the precipitate was collected, washed with a small amount of ether, and dried *in vacuo* at 150 °C (Found: C, 47.6; H, 3,45; N, 12.3. Calc. for $C_{42}H_{34}F_{12}N_{10}P_2Ru$: C, 47.2; H, 3.35; N, 13.0%).

Physical Measurements.—The UV/VIS spectra were obtained on a Perkin Elmer Lambda-3B or Hitachi U-3210 spectrophotometer, luminescence spectra on a Perkin Elmer 204A spectrofluorimeter, and Fourier-transform NMR spectra on a Varian XL400, XL300 or JEOL JEM-GX200 spectrometer. Electrochemical measurements were made with a three-electrode cell configuration controlled with a PAR 173 potentiostat, a PAR 176 i/E converter, and a PAR-175 waveform generator or a Yanagimoto model P-1100 voltammetric analyser. The working electrode was a glassy-carbon disk or platinum bead and the auxiliary electrode was a platinum foil or gauze. The reference electrode was a BAS RE-1 Ag–AgCl or an $Ag–Ag^+$ (0.01 mol dm^{-3} in 0.1 mol dm^{-3} NEt_4ClO_4–MeCN), the potential of the latter being +0.30 V with respect to the saturated calomel electrode (SCE).[9] All potentials are reported *vs.* SCE. The pH measurements were made with a TOA model HM-20E pH meter standardized with buffers of pH 4.01 and 6.89. Acetonitrile–water (1:1 v/v) was employed as solvent because of the limited solubility of the complexes in purely aqueous solution, particularly at the middle of our pH range. The glass-electrode pH readings from this mixture are referred to as 'pH' unless otherwise stated. Spectrophotometric titrations were also performed in acetonitrile–water (1:1 v/v), as described.[10] During the titrations, precipitation often occurred in the range pH 7–8, however this precipitate redissolved at higher pH. At higher pH (> 8) the complex is easily oxidized in contact with air, so the titrating solution was kept under an argon atmosphere and a little $Na_2S_2O_4$ was added as reductant.

Results and Discussion

Preparation of the Complexes.—The complexes $[RuL^7_2]^{2+}$ and $[RuL^8_2]^{2+}$ were prepared by reaction of the corresponding ligands with $RuCl_3{\cdot}3H_2O$, and characterized by elemental analysis and NMR spectroscopy.

Spectroscopic Properties.—(*a*) *NMR*. A representative ^1H NMR spectrum of $[RuL^7_2]^{2+}$ in $(CD_3)_2SO$ is shown in Fig. 1 and the data for the free ligands and their complexes are collected in Table 1, along with the co-ordination-induced shifts (c.i.s. = $\delta_{complex} - \delta_{ligand}$) in parentheses. The spectrum of the free ligand L^7 consists mainly of four sets of signals, which can be assigned to H(2), H(1), H(6) [and H(9)], H(7) [and H(8)] protons in this order, from the low-frequency end (see Fig. 1 for atom numbering). The magnetic equivalence of H(6) and H(9), or H(7) and H(8), indicates that the NH imino-protons exchange rapidly on the NMR time-scale with water protons present in the solvent. On co-ordination to the ruthenium ion, the chemical shifts of H(1) and H(2) were shifted downfield, while on the other hand H(6), H(7), H(8) and H(9) all show upfield shifts, and furthermore the overlapped signals for H(6) and H(9), or H(7) and H(8), are split into their individual resonances. These assignments were confirmed by selected decoupling experiments.

The observed c.i.s. values can be attributed to several factors; *i.e.* an electron σ donation to the Ru^{II} *via* the nitrogen lone pair, back donation to the ligands, van der Waals interactions, and interligand through-space ring-current anisotropy.[11] A large negative c.i.s. value for the H(9) proton is due to the magnetic anisotropy induced by the proximate ring current, but there is a lesser influence on the H(6), H(7) and H(8). Metal-to-ligand π-back donation should also produce negative c.i.s. values. However, as the benzimidazole moiety has relatively high π*-orbital energies compared to those of pyridine the contribution of this effect is small. On the other hand, H(1) and H(2) are not affected by the through-space ring-current anisotropy. Thus, positive c.i.s. values for H(1) and H(2) arise from a σ effect based on electron donation to the Ru^{II} *via* the nitrogen lone pair. Comparing the chemical shifts for $[RuL^7_2]^{2+}$ with those of $[RuL^8_2]^{2+}$, the H(2) signal of $[RuL^8_2]^{2+}$ is the only aromatic one shifted further downfield (about 0.3 ppm) relative to that of $[RuL^7_2]^{2+}$. This result is interpretable in terms of steric interaction between the *N*-methyl group and the H(2) proton, and the methyl group of L^8 is complementarily shifted 0.27 ppm downfield (from δ 4.27) on co-ordination.

The ^{13}C NMR spectra exhibit 10 signals in the δ 110–155 region for the co-ordinated ligands in $[RuL^7_2]^{2+}$ (Table 1). The assignments of the signals were confirmed by ^{13}C-{^1H} two-dimensional correlation spectroscopy. The ^{13}C NMR c.i.s.

Table 1 Proton and ^{13}C NMR chemical shifts for the free ligands and their ruthenium complexes in $(CD_3)_2SO$[a]

	Pyridine ring		Benzimidazole ring				
Compound	H(1)	H(2)	H(6)	H(7)	H(8)	H(9)	NH or NCH_3
L^7	8.19	8.36	7.77	7.33	7.33	7.77	13.03[b]
L^8	8.21	8.41	7.70	7.31	7.38	7.78	4.27
$[RuL^7_2]^{2+}$	8.80	8.93	7.59	7.25	7.02	6.05	13.03[b]
	(0.61)	(0.57)	(−0.11)	(−0.12)	(−0.31)	(−1.74)	
$[RuL^8_2]^{2+}$	8.70	9.12	7.74	7.31	7.03	6.05	4.51
	(0.49)	(0.71)	(0.04)	(0.00)	(−0.35)	(−1.73)	

	Pyridine ring		Benzimidazole ring							
	C(1)	C(2)	C(3)	C(4)	C(5)	C(6)	C(7)	C(8)	C(9)	C(10)
L^7	139.16	121.36	147.67	150.40	139.23	115.72	122.96	122.96	115.72	139.23
L^8	138.37	122.38	149.22	149.62	137.02	110.79	124.93	123.19	119.43	142.04
$[RuL^7_2]^{2+}$	136.70	122.22	149.56	151.44	133.30	114.21	125.55	124.71	114.50	140.78
	(−2.46)	(0.86)	(1.89)	(1.04)	(−5.93)	(−1.51)	(2.59)	(1.75)	(−1.22)	(1.55)
$[RuL^8_2]^{2+}$	131.00	119.43	145.21	145.99	130.49	107.85	120.59	120.01	110.19	134.79
	(−7.37)	(−2.95)	(−4.01)	(−3.63)	(−6.53)	(−2.94)	(−4.34)	(−3.18)	(−9.24)	(−7.25)

[a] The value in parentheses are co-ordination-induced shifts: c.i.s. = $\delta_{complex} - \delta_{ligand}$. [b] Broad signal because of rapid exchange.

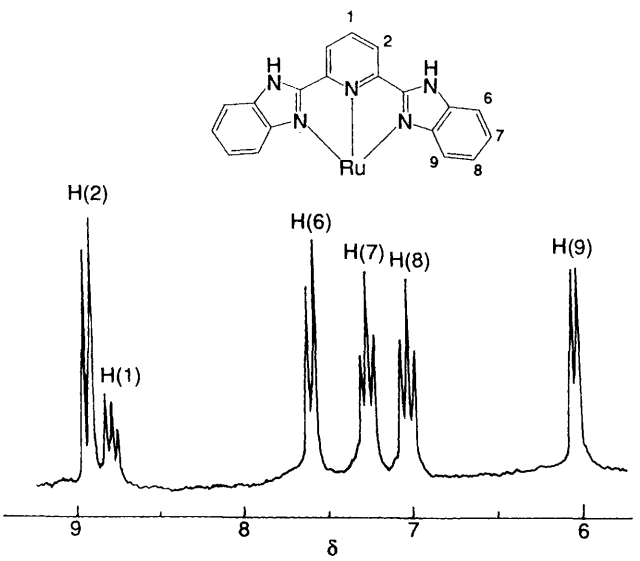

Fig. 1 Proton NMR spectrum of $[RuL^7_2]^{2+}$ in $(CD_3)_2SO$. The atom numbering is shown

values do not correlate in sign or magnitude with those for the ^1H NMR spectra because the relative contribution of the through-space ring-current anisotropy should be less important in ^{13}C than in ^1H NMR.[12] The relatively large negative c.i.s. values for carbons C(1), C(5), C(6) and C(9) indicate that metal-to-ligand π-back donation is predominant, whereas the other carbons show positive c.i.s. values, due mainly to ligand-to-metal σ donation.

In order to investigate the change in electronic states for $[RuL^7_2]^{2+}$ upon deprotonation, the ^1H and ^{13}C NMR chemical shifts in $(CD_3)_2SO$ were monitored during addition of tetraethylammonium hydroxide as a base (Fig. 2).* Although the ^1H signals of all protons are shifted upfield, the ^{13}C signals are divided into two groups, those with an upfield and those with a downfield shift. This is accounted for if all the protons are shielded in the ^1H NMR spectrum by an increase in the total charge of the complex through deprotonation. In the ^{13}C NMR spectra downfield shifts are observed for the carbons C(3)–C(6) and C(10), which shows that as expected the L^7 to metal σ donation is enhanced by deprotonation. On the other hand, the resonances of C(1), C(7) and C(8) in the L^7 ligand show an upfield shift, which reveals the larger shielding contribution based on the increase in electron density upon deprotonation. It can be concluded that the changes in the ^{13}C chemical shifts upon deprotonation parallel the changes in the other electronic properties of the co-ordinated ligands.

(*b*) *Optical spectra.* The optical spectral data are in Table 2. The ruthenium(II) chelates exhibit strong $d_{Ru} \longrightarrow \pi^*_{ligand}$ metal-to-ligand charge-transfer (m.l.c.t.) bands in the green and blue regions of the spectrum. The m.l.c.t. absorption maximum for $[RuL^7_2]^{2+}$ is observed at 475 nm in MeCN, which is almost comparable in energy to that of $[RuL^1_2]^{2+}$ and significantly lower compared to those of $[RuL^3_2]^{2+}$ and $[RuL^5_2]^{2+}$. In addition, $[RuL^7_2]^{2+}$ shows intense ligand π–π* bands at 355 and 315 nm, which are slightly diminished in intensity by co-ordination. The intraligand π–π* bands for $[RuL^1_2]^{2+}$ and $[RuL^5_2]^{2+}$ were observed at 310 and 285 nm, respectively. The differences in m.l.c.t. bands between $[RuL^5_2]^{2+}$ and $[RuL^7_2]^{2+}$ reflect the energy differences of the π* orbitals of the ligands. A longer-wavelength shift for $[RuL^8_2]^{2+}$ (λ_{max} 495 nm in MeCN) is observed compared to $[RuL^7_2]^{2+}$. The intraligand π–π* bands for both complexes are almost the same, whereas the d-orbital energy is raised by the stronger donor property of L^8 compared to L^7. The free ligands L^7 and L^8 are quite fluorescent at ambient temperature in MeCN, emitting in the near-UV region. However, the ruthenium(II) chelates exhibited no detectable ambient-temperature luminescence emission, apart from that presumably due to traces of free ligand. Many ruthenium(II) complexes with azaaromatic chelating agents (including benzimidazoles) are luminescent, even at room temperature, in association with m.l.c.t-excited ligand-localized emission.[1c,13] Therefore the emission from these benzimidazole-derived tridentate ligands is markedly quenched upon co-ordination. This apparently inverse relationship between the quantum yields of the free and co-ordinated ligands, though not necessarily a universal phenomenon, is reflected by similar results for at least some other ruthenium-chelates.[13]

(*c*) *Absorption spectroscopic titrations of* $[RuL^7_2]^{2+}$ *and free* L^7 *ligand.* The Lowry–Brønsted acid behaviour of the complex $[RuL^7_2]^{2+}$ causes its absorption spectra to be strongly pH dependent. In order to determine the pK_a values, direct spectrophotometric titration of $[RuL^7_2]^{2+}$ was performed in MeCN–buffer, as shown in Fig. 3. As the pH of the solution is raised from 2 to 8 the absorption maximum at 480 nm shifts to

* When the base : complex molar ratio was increased to 3 : 1, broadening of the resonances accompanied by a large shift occurred, suggesting the formation of a paramagnetic species by aerial oxidation of the complex.

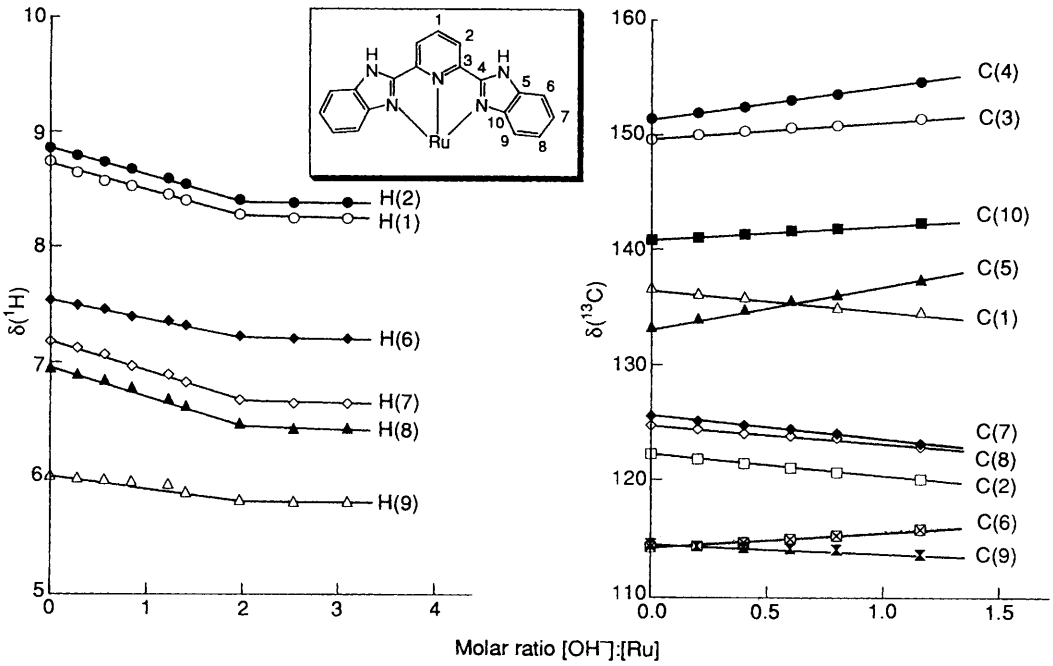

Fig. 2 The change in ^1H and ^{13}C NMR chemical shifts for $[RuL^7{}_2]^{2+}$ in $(CD_3)_2SO$ as a result of adding NEt_4OH. The atom numbering is shown

Table 2 Ambient-temperature optical spectroscopic data for the compounds[a]

Compound	λ/nm (10^{-3}ε/dm^3 mol^{-1} cm^{-1})
L^{7b}	325 (39.2)
	240 (sh) (26.2)
$[RuL^7{}_2][PF_6]_2$	475 (17.4)
	355 (56.6)
	315 (54.1)
	265 (45.9)
	205 (75.6)
L^{8c}	320 (39.1)
	240 (sh) (26.3)
	220 (sh) (61.4)
$[RuL^8{}_2][PF_6]_2$	490 (7.9)
	357 (66.7)
	343 (54.5)
	313 (42.8)
	305 (sh) (39.8)
	262 (42.7)
	246 (sh) (39.4)

[a] Spectra from MeCN solutions, deoxygenated for emission by bubbling nitrogen. [b] λ_{em} 370 (λ_{ex} 335 nm). [c] λ_{em} 370 (λ_{ex} 325 nm).

longer wavelength (492 nm), and a clean isosbestic point at 488 nm is observed. In the range pH 6.9–8.5 the absorption maximum at 492 nm then decreases, the subsequent increase of pH to 8.8–10.7 leads to the development of an absorption maximum at 506 nm. Plots of absorbance *vs.* pH at 480 and 506 nm are shown in Fig. 4. Since the $[RuL^7{}_2]^{2+}$ complex has four dissociable NH moieties, five equilibrium species are present throughout the pH region [see equation (2)], where $L^7 - H$ and $L^7 - 2H$ represent the mono- and di-deprotonated forms of L^7. Thus, the absorbance A of the ruthenium(II) complex can be expressed *via* equations (3)–(5) where ε_j, R_j and $[Ru^{II}]_T$ are the molar absorption coefficients, the concentrations of the

$$[Ru^{II}L^7{}_2]^{2+} \underset{H^+}{\overset{K_{11}}{\rightleftharpoons}} [Ru^{II}L^7(L^7 - H)]^{+} \underset{H^+}{\overset{K_{12}}{\rightleftharpoons}}$$

$$[Ru^{II}(L^7 - H)_2] \underset{H^+}{\overset{K_{13}}{\rightleftharpoons}} [Ru^{II}(L^7 - H)(L^7 - 2H)]^{-} \underset{H^+}{\overset{K_{14}}{\rightleftharpoons}}$$

$$[Ru^{II}(L^7 - 2H)_2]^{2-} \quad (2)$$

$$A = \sum_{j=1}^{5} \varepsilon_j R_j \quad (3)$$

$$R_j = [Ru^{II}]_T \left(\frac{K_{1,0} \cdots K_{1,(5-j)}}{[H^+]^{5-j}}\right)\left(\frac{1}{\alpha_{red}}\right) \quad (j = 1\text{–}5) \quad (4)$$

$$\alpha_{red} = 1 + \frac{K_{11}}{[H^+]} + \frac{K_{11}K_{12}}{[H^+]^2} + \frac{K_{11}K_{12}K_{13}}{[H^+]^3} + \frac{K_{11}K_{12}K_{13}K_{14}}{[H^+]^4} \quad (5)$$

ruthenium(II) species at the various degrees of protonation, and the total concentration of $[Ru^{II}L^7{}_2]^{2+}$, respectively. The $K_{1,(5-j)}$ values describe the acid dissociation constants for the $(5 - j)$th proton in the ruthenium(II) oxidation state; $K_{1,0}$ is defined as 1. The regression curves fitted to equations (3)–(5) are shown in Fig. 4 as solid and broken lines. The theoretical curves reproduced the absorbance *vs.* pH data well, and the $K_{1,(5-j)}$ values obtained are $pK_{11} = 6.42$, $pK_{12} = 7.20$, $pK_{13} = 8.70$ and $pK_{14} = 11.00$.

The free L^7 ligand itself can act as a Lowry–Brønsted acid which can be titrated. In aqueous ethanol solution (20:80 v/v), free L^7 has π–π* absorption bands in the 250–350 nm region. Increasing the pH leads to a distinct decrease in the intensity at 250 nm. From this spectral change the pK_a value for the first proton ionization [equation (6)] can be estimated as pK_a =

$$L^7 \longrightarrow (L^7 - H) + H^+ \quad (6)$$

11.5 ± 0.1. On co-ordination of L^7 to Ru^{II} a marked decrease in pK_a is observed for the first imino NH dissociation of L^7 (pK_a 11.5 becomes 5.7). In turn, when the oxidation state of ruthenium is changed from +2 to +3 the pK_a values are decreased by four units, clearly resulting from the larger electron-withdrawing ability of Ru in the higher oxidation state.

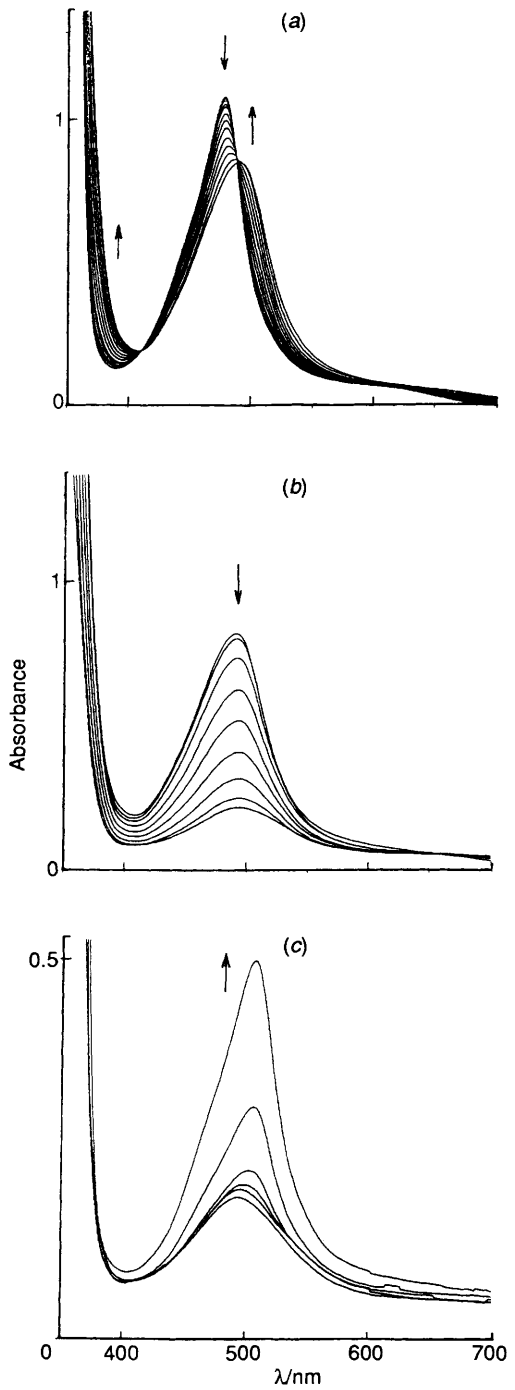

Fig. 3 Absorption spectra of $[RuL^7{}_2]^{2+}$ in MeCN–buffer (1 : 1 v/v) at pH 4.0–6.9 (*a*); 6.9–8.5 (*b*); and 8.8–10.7 (*c*). The absorbance scale in (*c*) is different from those of (*a*) and (*b*)

Electrochemistry.—(*a*) *In non-aqueous solvent.* The redox potentials are collected in Table 3, including data for other relevant ruthenium bis(tridentate ligand) complexes.[4,5] The complex $[RuL^7{}_2]^{2+}$ shows a reversible one-electron oxidation at +0.76 V *vs.* SCE in MeCN. *N*-Methylation of the four benzimidazole rings in $[RuL^7{}_2]^{2+}$ causes $E_{\frac{1}{2}}(Ru^{III}–Ru^{II})$ to shift cathodically. The reduction processes for $[RuL^7{}_2]^{2+}$ are irreversible in MeCN and complicated by adsorption and/or chemical reactions coupled to the electron transfer. However, $[RuL^8{}_2]^{2+}$ exhibits two Nernstian one-electron reduction processes at −1.40 and −1.72 V *vs.* SCE in MeCN. Replacement of the two pyridine rings of terpy or the two pyrazole rings

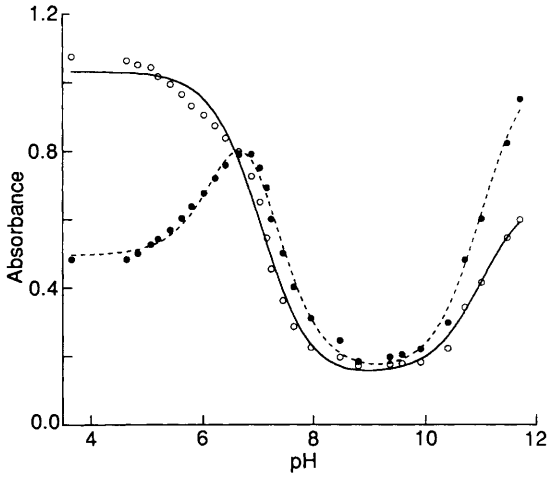

Fig. 4 Spectroscopic titration curves of $[RuL^7{}_2]^{2+}$ at 480 (○) and 506 nm (●) *vs.* pH in MeCN–buffer (1 : 1 v/v); —— and – – –, regression curves based on equations (3)–(5). See text for details

of L^3 with two benzimidazole rings leads to a +0.5 V cathodic shift of the $Ru^{III}–Ru^{II}$ potential, suggesting a stronger donor ability for the L^7 ligand.

(*b*) *Proton-coupled electron-transfer processes in* MeCN–*buffer.* The pK_a values for different oxidation states, such as those for Ru^{II}-and Ru^{III}-linked ionizations, can be obtained by analysing the $E_{\frac{1}{2}}$ *vs.* pH (Pourbaix) diagram. Fig. 5 shows typical oxidative voltammograms for $[RuL^7{}_2]^{2+}$ at pH 4.29 in MeCN–buffer (1 : 1 v/v). Two well defined waves are observed. Each is a reversible one-electron oxidation process (ΔE_p = 70 ± 10 mV; $E_{\frac{1}{2}}$ independent of scan rate). By analogy with other ruthenium(II) complexes, the first wave is assigned to the $Ru^{III}–Ru^{II}$ couple, and the second, higher-potential one to the $Ru^{IV}–Ru^{III}$ couple. A plot of the half-wave potential, $E_{\frac{1}{2}}$, *vs.* pH is shown in Fig. 6. Below pH 2.0 and above pH 10.5, the $Ru^{III}–Ru^{II}$ couple is independent of pH. Over the range pH 2.0–10.5 the $E_{\frac{1}{2}}$ value decreases linearly with increasing pH. The slopes for this line gradually change through −60, −120, −180, −120 and −60 mV per pH unit in the ranges pH 2.5–3.2, 3.2–5.1, 5.1–7.8, 7.8–9.1 and 9.1–10.7, respectively.

Since the existence of five equilibrium species has been demonstrated by the spectrophotometric titration, the electrode processes for the $Ru^{III}–Ru^{II}$ couple can be described in terms of Scheme 1, involving both redox and acid–base equilibria. The

$$[Ru^{II}L^7{}_2]^{2+} \underset{e^-}{\rightleftharpoons} [Ru^{III}L^7{}_2]^{3+}$$

$$H^+ \Big\| K_{11} \qquad H^+ \Big\| K_{21}$$

$$[Ru^{II}L^7(L^7 - H)]^+ \underset{e^-}{\rightleftharpoons} [Ru^{III}L^7(L^7 - H)]^{2+}$$

$$H^+ \Big\| K_{12} \qquad H^+ \Big\| K_{22}$$

$$[Ru^{II}(L^7 - H)_2] \underset{e^-}{\rightleftharpoons} [Ru^{III}(L^7 - H)_2]^+$$

$$H^+ \Big\| K_{13} \qquad H^+ \Big\| K_{23}$$

$$[Ru^{II}(L^7 - H)(L^7 - 2H)]^- \underset{e^-}{\rightleftharpoons} [Ru^{III}(L^7 - H)(L^7 - 2H)]$$

$$H^+ \Big\| K_{14} \qquad H^+ \Big\| K_{24}$$

$$[Ru^{II}(L^7 - 2H)_2]^{2-} \underset{e^-}{\rightleftharpoons} [Ru^{III}(L^7 - 2H)_2]^-$$

Scheme 1

Table 3 Electrochemical data for the ruthenium complexes in MeCN[a]

Complex	Oxidation	Reduction	Ref.
$[RuL^1{}_2]^{2+}$	+1.27	−1.27, −1.51	4(*e*)
$[RuL^2{}_2]^{2+}$	+1.25	−1.24	4(*f*)
$[RuL^3{}_2]^{2+}$	+1.25	−1.66[b]	5
$[RuL^4{}_2]^{2+}$	+1.16	−1.35, −1.58	4(*e*)
$[RuL^5{}_2]^{2+}$	+1.06	−1.90,[b] −2.20[b]	4(*h*)
$[RuL^6{}_2]^{2+}$	+1.406	−0.831, −1.096, −1.474, −1.719	4(*b*)
$[RuL^7{}_2]^{2+}$	+0.76 (53)	−1.70[b]	This work
$[RuL^8{}_2]^{2+}$	+0.70 (61)	−1.40 (62), −1.72 (80)	This work

[a] In volts *vs.* SCE. The values in parentheses are the peak separations in mV. [b] Peak potential, irreversible.

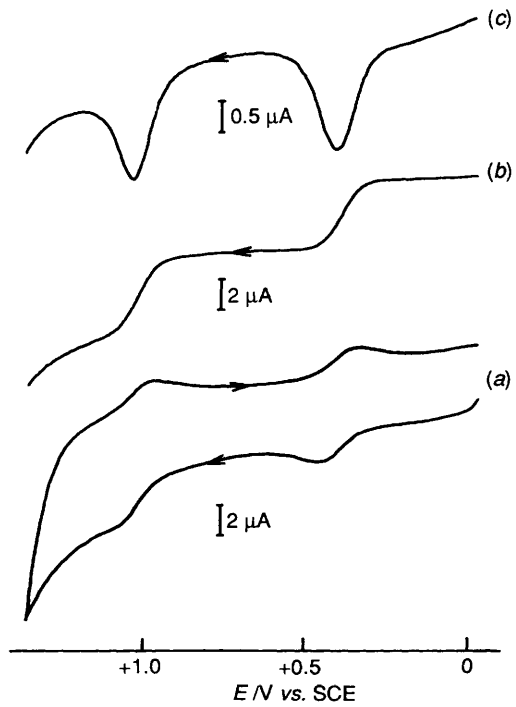

Fig. 5 Cyclic (*a*), rotating disk (*b*) and differential pulse (*c*) voltammograms for $[RuL^7{}_2]^{2+}$ at pH 4.29 in MeCN–buffer (1 : 1 v/v) at a glassy carbon electrode

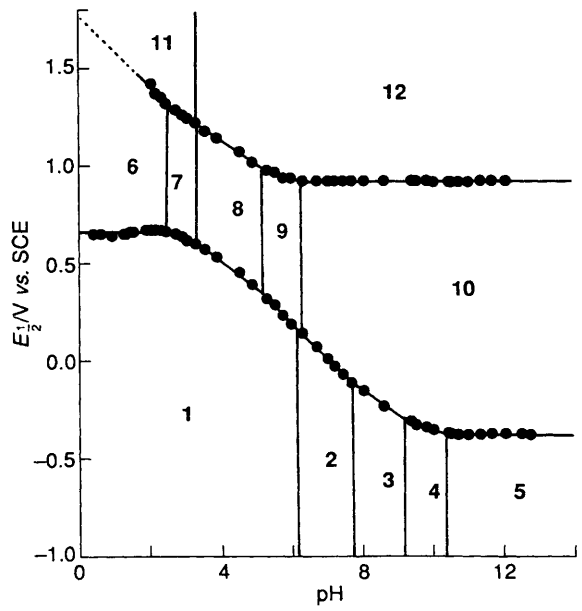

Fig. 6 The half-wave potential, $E_{\frac{1}{2}}$, *vs.* pH for $[RuL^7{}_2]^{2+}$ in MeCN–buffer (1 : 1 v/v) at 25 °C: **1**, $[Ru^{II}L^7{}_2]^{2+}$; **2**, $[Ru^{II}L^7(L^7 - H)]^+$; **3**, $[Ru^{II}(L^7 - H)_2]$; **4**, $[Ru^{II}(L^7 - H)(L^7 - 2H)]^-$; **5**, $[Ru^{II}(L^7 - 2H)_2]^{2-}$; **6**, $[Ru^{III}L^7{}_2]^{3+}$; **7**, $[Ru^{III}L^7(L^7 - H)]^{2+}$; **8**, $[Ru^{III}(L^7 - H)_2]^+$; **9**, $[Ru^{III}(L^7 - H)(L^7 - 2H)]$; **10**, $[Ru^{III}(L^7 - 2H)_2]^-$; **11**, $[Ru^{IV}(L^7 - H)(L^7 - 2H)]^+$; **12**, $[Ru^{IV}(L^7 - 2H)_2]$

notation for the complexes is the same as that in equation (2). The pH dependence of $E_{\frac{1}{2}}$ can be expressed as in equations (7)–(9),[14] where $E_{\frac{1}{2}}^\circ$ is the standard redox potential of the

$$E_{\frac{1}{2}} = E_{\frac{1}{2}}^\circ + \frac{RT}{F}\ln\left(\frac{\alpha_{red}}{\alpha_{ox}}\right) \quad (7)$$

$$\alpha_{ox} = 1 + \frac{K_{21}}{[H^+]} + \frac{K_{21}K_{22}}{[H^+]^2} + \frac{K_{21}K_{22}K_{23}}{[H^+]^3} + \frac{K_{21}K_{22}K_{23}K_{24}}{[H^+]^4} \quad (8)$$

$$\alpha_{red} = 1 + \frac{K_{11}}{[H^+]} + \frac{K_{11}K_{12}}{[H^+]^2} + \frac{K_{11}K_{12}K_{13}}{[H^+]^3} + \frac{K_{11}K_{12}K_{13}K_{14}}{[H^+]^4} \quad (9)$$

$[Ru^{III}L^7{}_2]^{3+}$–$[Ru^{II}L^7{}_2]^{2+}$ couple at pH 0. The K_{nm} values describe the acid dissociation constants for the *m*th proton in the ruthenium oxidation state $n + 1$. Non-linear regression analysis of the $E_{\frac{1}{2}}$ *vs.* pH data was carried out according to the above model, yielding pK_a values for both oxidation states II and III: $pK_{11} = 6.10$, $pK_{12} = 7.80$, $pK_{13} = 9.10$ and $pK_{14} = 10.70$, and $pK_{21} = 2.50$, $pK_{22} = 3.20$, $pK_{23} = 5.10$ and $pK_{24} = 6.20$ respectively.

Similarly, the electrode processes for the Ru^{IV}–Ru^{III} couple were also analysed, using Scheme 2. The pK_a values for the III oxidation state, pK_{21}–pK_{24}, in Scheme 2 should be consistent with those obtained from the analysis of $E_{\frac{1}{2}}$ *vs.* pH plots for Ru^{III}–Ru^{II} couple described above. Performing the data analysis for the Ru^{IV}–Ru^{III} process in such a self-consistent manner, only two species, $[Ru^{IV}(L^7 - 2H)_2]$ and $[Ru^{IV}(L^7 - H)(L^7 - 2H)]^+$, can be seen within the range pH 0–12 for the IV oxidation state, and the fourth acid dissociation constant, pK_{34} can be determined as 3.1. The pK_a values for various oxidation states are summarized in Table 4.

The redox potential can be altered by more than a volt by changing the pH value from 2 to 10. The reactivity of the complex toward aerial oxygen is thus dramatically changed; the II state is stable at pH 2, but oxidation by air occurs readily at pH 10. Fig. 7 shows the absorption spectral change for $[RuL^7{}_2]^{2+}$ when in contact with air at pH 10. The absorption maximum at 506 nm decreases and a new peak at 570 nm gradually appears with time. The ruthenium(III) complex formed is easily re-reduced to the original ruthenium(II) state by reaction with $S_2O_4^{2-}$. The initial reaction, which proceeds as a result of the significant decrease in reduction potential caused by deprotonation, may be expressed as in equation (10). Thus,

Table 4 pK_a Values obtained for co-ordinated ligands in ruthenium complexes for various oxidation states in MeCN–buffer (1:1 v/v) at 25 °C[a]

	pK_a			
Complex	1st	2nd	3rd	4th
L^7	(11.5)[b]			
$[RuL^7{}_2]^{z+}$				
$Ru^{II}(z = 2)$	6.1	7.8	9.1	10.7
	(6.42)	(7.20)	(8.70)	(11.00)
$Ru^{III}(z = 3)$	2.5	3.2	5.1	6.2
$Ru^{IV}(z = 4)$	< 0	< 0	< 2	3.1
$[Ru(bipy)_2(H_2bbzim)]^{z+}$[c]				
$Ru^{II}(z = 2)$	5.74	10.51		
$Ru^{III}(z = 3)$	0.55	6.60		

[a] The values in parentheses are those obtained spectrophotometrically. [b] Measured in aqueous ethanol (20:80 v/v). [c] Ref. 10(*a*).

$$[Ru^{III}L^7{}_2]^{3+} \underset{e^-}{\rightleftharpoons} [Ru^{IV}L^7{}_2]^{4+}$$

$$H^+ \downarrow\uparrow K_{21} \qquad H^+ \downarrow\uparrow K_{31}$$

$$[Ru^{III}L^7(L^7 - H)]^{2+} \underset{e^-}{\rightleftharpoons} [Ru^{IV}L^7(L^7 - H)]^{3+}$$

$$H^+ \downarrow\uparrow K_{22} \qquad H^+ \downarrow\uparrow K_{32}$$

$$[Ru^{III}(L^7 - H)_2]^+ \underset{e^-}{\rightleftharpoons} [Ru^{IV}(L^7 - H)_2]^{2+}$$

$$H^+ \downarrow\uparrow K_{23} \qquad H^+ \downarrow\uparrow K_{33}$$

$$[Ru^{III}(L^7 - H)(L^7 - 2H)] \underset{e^-}{\rightleftharpoons} [Ru^{IV}(L^7 - H)(L^7 - 2H)]^+$$

$$H^+ \downarrow\uparrow K_{24} \qquad H^+ \downarrow\uparrow K_{34}$$

$$[Ru^{III}(L^7 - 2H)_2]^- \underset{e^-}{\rightleftharpoons} [Ru^{IV}(L^7 - 2H)_2]$$

Scheme 2

$$[Ru^{II}\{L^7 - (2 - p)H\}_2]^{(2p-2)+} + O_2 \longrightarrow [Ru^{III}\{L^7 - (2 - p)H\}_2]^{(2p-1)+} + O_2^- \quad (10)$$

in alkaline solution above pH 8.0, the complex is stabilized in the III oxidation state in the presence of oxygen.

Redox Tuning of $[Ru^{II}L^7{}_2]^{2+}$ *by Outer-sphere Interactions.*—It appears that the half-wave potential of $[Ru^{II}L^7{}_2]^{2+}$ is solvent dependent; the value for the Ru^{III}–Ru^{II} couple shifts cathodically when a solvent with a larger donor number is used. We suggest that the lowering of the potential is due to a specific hydrogen-bond acceptor interaction. A similarly negative potential shift for the oxidation of $[Ru(H_2bbzim)_3]^{2+}$ (H_2bbzim = 2.2′-bibenzimidazole) in different solvents has been reported.[15] It may therefore be generally true that all such complexes with benzimidazole or imidazole ligands exhibit solvent effects on their redox potentials due to specific interactions between the complex and the solvent.

The Influence of Proton Dissociation.—The ionization of the four protons in $[RuL^7{}_2]^{2+}$ causes about a 1.0 V negative shift of the redox potential. This large shift arises from the greater σ-donor ability of $[L^7 - 2H]^{2-}$, formed by the deprotonation of L^7. It makes the complex easily oxidized by oxygen, and even leads to stabilization of the IV oxidation state of the ruthenium through deprotonation. Recently, we reported a similar high-oxidation-state stabilization by NH imino deprotonation, in $[Ru(bipy)_2(H_2bbzim)]^{2+}$.[10a] Moreover, proton transfer-coupled electron transfer in the Ru(=O)–$Ru(OH_2)$ couple has been reported, in which the high (V and IV) oxidation states can be accessed *via* quite mild oxidants.[16]

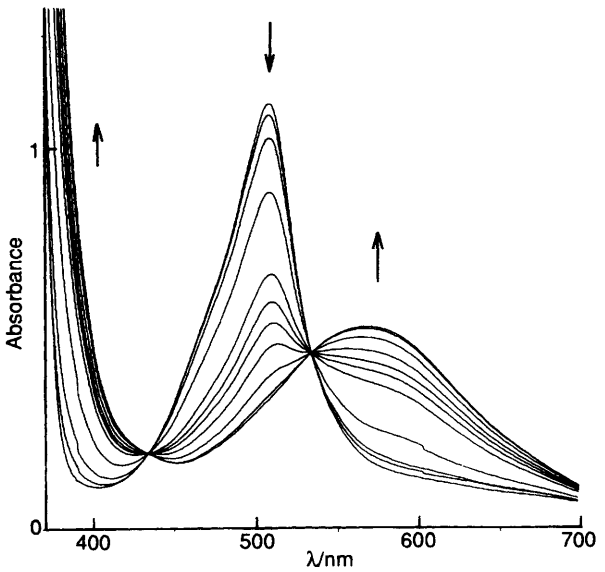

Fig. 7 Time course of the absorption spectral change of $[RuL^7{}_2]^{2+}$ at pH 10 upon reaction with air. Each spectrum was recorded at 2 min intervals

Acknowledgements

This work was partially supported by a Grant-in-Aid for Scientific Research (No. 04453045) from the Ministry of Education and the basic science fund from the Sumitomo Foundation (for M. H.). M. H. thanks Mr. Tomoaki Ano for experimental assistance at the initial stage of this work. The Japan–China Teacher Exchange Program fellowship enabling X. X. from Hunan Normal University to spend a year's leave in Japan is also gratefully acknowledged, and we also thank Drexel University for support.

References

1 (*a*) E. A. Seddon and K. R. Seddon, *The Chemistry of Ruthenium*, Elsevier, Amsterdam, 1984; (*b*) K. Kalyanasundaram, *Coord. Chem. Rev.*, 1989, **28**, 2920; (*c*) A. Juris, V. Balzani, F. Barigelletti, S. Campagna, P. Belser and A. von Zelewsky, *Coord. Chem. Rev.*, 1988, **84**, 85; (*d*) T. J. Meyer, *Acc. Chem. Res.*, 1989, **22**, 163; (*e*) V. Balzani and F. Scandola, *Supramolecular Photochemistry*, Ellis Horwood, Chichester, 1991.
2 A. B. P. Lever, *Inorg. Chem.*, 1990, **29**, 1271.
3 E. C. Constable, *Adv. Inorg. Chem. Radiochem.*, 1986, **30**, 69.
4 (*a*) J.-P. Sauvage and M. Ward, *Inorg. Chem.*, 1991, **30**, 3869; (*b*) S. Campagna, A. Mamo and J. K. Stille, *J. Chem. Soc., Dalton Trans.*, 1991, 2545; (*c*) E. C. Constable, R. P. G. Henney, T. A. Leese and D. A. Tocher, *J. Chem. Soc., Dalton Trans.*, 1990, 443; (*d*) E. C. Constable and M. D. Ward, *J. Chem. Soc., Dalton Trans.*, 1990, 1405; (*e*) A. J. Downard, G. E. Honey and P. J. Steel, *Inorg. Chem.*, 1991, **30**, 3733; (*f*) J.-P. Collin, S. Guillerez, J.-P. Sauvage, F. Barigelletti, L. De Cola, L. Flamigni and V. Balzani, *Inorg. Chem.*, 1991, **30**, 4230; (*g*) F. R. Keene, D. J. Szalda and T. A. Wilson, *Inorg. Chem.*, 1987, **26**, 2211; (*h*) S. Mahapatra and R. Mukherjee, *J. Chem. Soc., Dalton Trans.*, 1992, 2337; (*i*) E. C. Constable and A. M. W. C. Thompson, *J. Chem. Soc., Dalton Trans.*, 1992, 3467.
5 D. L. Jameson, J. K. Blaho, K. T. Kruger and K. A. Goldsby, *Inorg. Chem.*, 1989, **28**, 4312.
6 H. Nishiyama, H. Sakaguchi, T. Nakamura, M. Horihata, M. Kondo and K. Itoh, *Organometallics*, 1989, **8**, 846; D. A. Evans, K. A. Woerpel, M. M. Hinman and M. M. Faul, *J. Am. Chem. Soc.*, 1991, **113**, 726; E. J. Corey, N. Imai and H.-Y. Zhang, *J. Am. Chem. Soc.*, 1991, **113**, 728.

7 A. Dovletoglou, S. A. Adeyemi, M. H. Lynn, D. J. Hodgson and T. J. Meyer, *J. Am. Chem. Soc.*, 1990, **112**, 8989 and refs. therein.
8 A. W. Addison and P. Burke, *J. Heterocycl. Chem.*, 1981, **18**, 803; A. W. Addison, T. N. Rao and C. G. Wahlgren, *J. Heterocycl. Chem.*, 1983, **20**, 1481; C. Piguet, G. Bernardinelli and A. F. Williams, *Inorg. Chem.*, 1989, **28**, 2920; S. B. Sanni, H. J. Behm, P. T. Beurskens, G. A. van Alberda, J. Reedijk, A. T. H. Lenstra, A. W. Addison and M. Palaniandavar, *J. Chem. Soc., Dalton Trans.*, 1988, 1429; A. W. Addison, S. Burman, C. G. Wahlgren, O. A. Rajan, T. M. Rowe and E. Sinn, *J. Chem. Soc., Dalton Trans.*, 1987, 2621.
9 A. W. Addison, T. H. Li and L. S. Weiler, *Can. J. Chem.*, 1977, **55**, 766.
10 (*a*) A. M. Bond and M. Haga, *Inorg. Chem.*, 1986, **25**, 4507; (*b*) M. Haga, T. Ano, K. Kano and S. Yamabe, *Inorg. Chem.*, 1991, **30**, 3843.
11 G. Orellana, C. A. Ibarra and J. Santoro, *Inorg. Chem.*, 1988, **27**, 1025.
12 P. J. Steel and E. C. Constable, *J. Chem. Soc., Dalton Trans.*, 1990, 1389.
13 M. R. McDevitt, R. Yu and A. W. Addison, *Transition Met. Chem.*, 1993, **18**, 197.
14 W. M. Clark, *Oxidation-Reduction Potentials of Organic Systems*, Williams & Wilkins, Baltimore, MD, 1960, ch. 4.
15 M. Haga, *Inorg. Chim. Acta*, 1983, **77**, L39.
16 K. J. Takeuchi, M. S. Thompson, D. W. Pipes and T. J. Meyer, *Inorg. Chem.*, 1984, **23**, 1845.

Received 26*th January* 1993; *Paper* 3/00478C